JPn

Neuroscience

Bi-directional modulation of somatosensory mismatch negativity with transcranial direct current stimulation: an event related potential study

Jui-Cheng Chen[1,2,3], Dorothea Hämmerer[4], Kevin D'Ostilio[5], Elias P. Casula[1,6], Louise Marshall[1], Chon-Haw Tsai[2,3], John C. Rothwell[1] and Mark J. Edwards[1]

[1] *Sobell Department of Motor Neuroscience and Movement Disorders, UCL Institute of Neurology, Queen Square, London, WC1N 3BG, UK*
[2] *Neuroscience Laboratory, Department of Neurology, China Medical University Hospital, Taichung, Taiwan*
[3] *School of Medicine, China Medical University, Taichung, Taiwan*
[4] *Department of Psychology, TU Dresden, Dresden, Germany*
[5] *MoVeRe Group, Cyclotron Research Centre, University of Liege, Belgium*
[6] *Lifespan Cognitive Neuroscience Laboratory, Department of General Psychology, University of Padua, Via Venezia 8, Padua 35131, Italy*

The Journal of Physiology

Key points

- Sensory mismatch negativity is impaired in patients with cerebellar lesions, suggesting that the cerebellum may play an important role in this form of sensory processing.
- Anodal transcranial direct current stimulation over the right cerebellar hemisphere increased the amplitude of sensory mismatch negativity to stimuli delivered to the right hand while cathodal transcranial direct current stimulation reduced it.
- The cerebellum appears to be an important node in the network mediating sensory mismatch negativity, and tDCS is a useful method with which to manipulate sensory mismatch negativity for experimental studies.

Abstract Appropriate orientation towards potentially salient novel environmental stimuli requires a system capable of detecting change in the sensorium. Mismatch negativity (MMN), an evoked potential calculated by subtracting the response to a standard repeated stimulus and a rare 'oddball' stimulus, is proposed as such a change detection mechanism. It is most widely studied in the auditory domain, but here we chose to explore the mechanism of somatosensory MMN, and specifically its dependence on the cerebellum. We recorded event-related potentials (ERPs) evoked in response to auditory and sensory stimuli from 10 healthy subjects before and after anodal, cathodal and sham transcranial direct current stimulation (tDCS) of the right cerebellar hemisphere. There was a significant increase in peak amplitude of somatosensory MMN after anodal tDCS ($F_{(1,9)} = 8.98$, $P < 0.02$, mean difference anodal pre–post: $-1.02\ \mu$V) and a significant reduction in peak amplitude of somatosensory MMN after cathodal tDCS ($F_{(1,9)} = 7.15$, $P < 0.03$, mean difference cathodal pre–post: $0.65\ \mu$V). The amplitude of auditory MMN was unchanged by tDCS. These results reveal the capability of tDCS to cause bidirectional modulation of somatosensory MMN and the dependence of somatosensory MMN on the cerebellum.

Introduction

It would be hard to function successfully in the environment without a method to filter or suppress the majority of the sensory stimuli that compete for our attention at any one time. However, it is equally true that it is advantageous to have a mechanism to detect salient change in the environment and to 'involuntarily' orientate our attention towards this potentially important stimulus. Mismatch negativity (MMN) is a negative component of the event related potential (ERP; Sams *et al.* 1985), calculated by subtracting the ERP from a repeatedly presented stimulus ('standard') from a rarely presented stimulus ('oddball'), and seems a strong candidate mechanism for the involuntary biasing of attention towards a potentially salient change in the sensory environment. For example, MMN can be recorded for auditory stimuli which infrequently differ in frequency or duration, or for more complex situations such as the absence of an expected tone (Sams *et al.* 1985; Paavilainen *et al.* 1989; Tervaniemi *et al.* 1994; Yabe *et al.* 1997). A model of interconnected structures (primary auditory cortex, superior temporal gyrus, inferior frontal gyrus) has been proposed to explain the generation of auditory MMN with the suggestion that plastic changes caused by repeated presentation of a stimulus (adaptation – perhaps most important at lower hierarchical levels) and comparison of current input with a memory trace of previous input (model adjustment – perhaps most important at higher hierarchical levels) are both mechanisms that underlie the production of MMN (Friston *et al.* 2003; Naatanen *et al.* 2005, 2007; Garrido *et al.* 2007, 2008, 2009). There is interest clinically in the MMN given its abnormality (typically absence) in a number of neurological/neuropsychiatric disorders, most notably schizophrenia (Umbricht *et al.* 2003), but also dyslexia (Baldeweg *et al.* 1999) and in patients with more general learning difficulties (Mowszowski *et al.* 2012). MMN may also be of relevance to the diagnosis and prediction of recovery for patients in persistent vegetative states and other states of altered consciousness (Wijnen *et al.* 2007).

While MMN has been most intensively studied in the auditory domain, it is also reported in the visual and sensory domains (Alho *et al.* 1992; Kekoni *et al.* 1997; Shinozaki *et al.* 1998; Akatsuka *et al.* 2005; Spackman *et al.* 2007, 2010; Butler *et al.* 2011, 2012). In the sensory domain it has been assessed most commonly using vibrotactile sensation (for example with different durations of stimulation or different frequencies of stimulation for standard and oddball stimuli; Kekoni *et al.* 1997; Spackman *et al.* 2007, 2010; Butler *et al.* 2011). An alternative method recently described is to use an electrical stimulus delivered to the index finger or little finger (Akatsuka *et al.* 2005; Restuccia *et al.* 2007, 2009). However, there is not yet a clear understanding of the structures involved in the production of sensory MMN.

Restuccia *et al.* have studied somatosensory MMN in patients with unilateral cerebellar hemisphere stroke, and found absent sensory MMN ipsilateral to the lesion, but normal auditory MMN (Restuccia *et al.* 2007). Here we aim to confirm and extend this observation in healthy subjects using non-invasive electrical stimulation of the cerebellum. Transcranial direct current stimulation (tDCS) is thought to alter cerebellar excitability (Galea *et al.* 2009; Hamada *et al.* 2012) through changes in Purkinje cell activity, and we hypothesized that different polarities of stimulation which are known to cause opposing plastic effects would have differential effects on the amplitude of sensory MMN.

Methods

Ethical approval

The studies described here conformed to the standards set by the *Declaration of Helsinki*, and all of the procedures were approved by the National Hospital of Neurology and Neurosurgery and the Institute of Neurology Research Ethics Committee, UK. All subjects gave their written informed consent to participate in the study.

Experiment 1

Subjects. We studied 10 subjects (4 men and 6 women, mean age 57.5 years; range 49–72 years). Subjects were without a history of major neurological or other illness and were not taking medication at the time of the study. Each subject was assessed on three different occasions (anodal tDCS, cathodal tDCS and sham tDCS), and each experimental session was randomized between subjects and separated by at least 7 days. Somatosensory MMN was assessed before and immediately after anodal tDCS, cathodal tDCS and sham stimulation.

MMN. Our initial aim was to use the spatial discrimination MMN technique described by Restuccia *et al.* but (see Results) we were unable to record reliable MMN using this technique. We therefore reassessed subjects using the vibrotactile technique reported by others.

Spatial discrimination somatosensory MMN. Somatosensory stimuli were delivered via electrodes (Ag–AgCl) placed on the right first and fifth fingers. Stimulation (square-wave pulse; stimulus duration, 0.2 ms) was applied at an intensity of just above the perceptual threshold (mean 2.96 mA, range 2.4–3.5 mA) using a constant current generator (Digitimer, Welwyn Garden

City, UK). Anodes were placed above the distal phalanx and cathodes put above the proximal phalanx. Simulation was delivered to 1st and 5th fingers with a proportion of 80% and 20%, respectively, in a pseudorandom fashion. There were two blocks of stimulation, with each block containing 500 trials with an interstimulus interval of 1000 ms and an inter-block interval of 2 min (Restuccia *et al.* 2007).

Vibratory somatosensory MMN. Vibratory stimuli were delivered via an electromagnetic mechanical stimulator (Ling Dynamics Systems, Skogsborgvej, Denmark) with a 3 cm-diameter circular probe grasped in the palm of the right hand. The probe was positioned orthogonally to, and under slight pressure against, the palm of the right hand. Stimulation was applied at an amplitude of 0.2–0.5 mm and a frequency of 70 Hz (Kassavetis *et al.* 2012). Stimuli differed in duration between standard and oddball stimuli (30 ms and 150 ms, respectively), presented pseudorandomly with proportions of 80% and 20%, respectively. The experiment consisted of one block of 500 trials with an interstimulus interval of 1000 ms. All subjects wore earphones to prevent auditory evoked potentials from the noise of the vibrator.

Experiment 2

Subjects. We studied 10 subjects (8 men and 2 women, mean age 32 years; range 23–38 years). Subjects were without a history of major neurological or other illness and were not taking medication at the time of the study. Each subject was assessed on three different occasions (anodal tDCS, cathodal tDCS and sham tDCS), and each experimental session was separated by at least 7 days. Auditory MMN was assessed before and immediately after anodal tDCS, cathodal tDCS and sham stimulation.

Auditory MMN. Auditory stimuli were delivered via a single speaker placed 0.5 m in front of subjects. In order to ensure that the stimuli were clearly audible, the intensity was set at 65 dB which was considerably above the auditory threshold of all subjects. The experiment consisted of two blocks of auditory MMN. Each block included 500 trials; blocks were separated by 2 min. Auditory stimuli of two different durations (50 ms and 100 ms) at a constant frequency of 333 Hz were delivered pseudorandomly in different proportions (80% and 20%, respectively). The interstimulus interval was 0.51 s.

Transcranial direct current stimulation

Electric stimulation was applied via two saline-rinsed sponges of 5 cm × 5 cm. The anodal electrode was placed over the right cerebellar cortex, 3 cm lateral to the inion. The other electrode was positioned on the right buccinators muscle for anodal stimulation while the cathodal electrode was placed over right cerebellar hemisphere and the reference electrode placed over the right buccinators for the cathodal stimulation, in accordance with the method used by Galea *et al.* (2009). The stimulation intensity was 2 mA, and stimulation duration was set to 25 min. Sham stimulation was applied with the sponges placed in the same position, but with stimulation stopped after 30 s. At the onset of all interventions (anodal, cathodal and sham), the current had a ramp-up time of 10 s, was held at 2 mA for 25 min, and then ramped down over 10 s.

EEG recordings and processing

Subjects sat on a comfortable chair with their hands supported on a pillow. A video with no sound was played during the experiment with the monitor placed 0.5 m away from the subjects. Thirty-two Ag–AgCl scalp electrodes (Fp1, Fpz, Fp2, F7, F3, Fz, F4, F8, FC5, FC1, FCz, FC2, FC6, M1, T7, C3, Cz, C4, T8, M2, CP5, CP1, CP2, CP6, P7, P3, Pz, P4, P8, O1, Oz, O2), placed according to the 10–20 system, were used for the electroencephalogram (EEG) recording. Electrode impedance was kept below 5 kΩ. The reference electrode was placed on bilateral mastoids, M1 reference was used for online recording and bilateral M1 + M2 for offline analysis. During recording, the sampling rate was set at 512 Hz, and data were online filtered with a 0.3–100 Hz bandpass filter. After recording, the data were bandpass-filtered at 1–30 Hz. Epochs of −50 to 500 ms were extracted using EEGLab V.11 software (http://sccn.ucsd.edu/eeglab/). Baseline correction was applied in a time window 50 ms prior to stimulus onset. Artefacts exceeding 100 μV were automatically rejected; artefact-free EEG sweeps were averaged per individual and the MMN was calculated by subtraction of 'oddball' from 'standard' ERPs.

Analysis

Data were analysed using SPSS (version 20.0). Averaged mismatch negativity waveforms of the pre- or post-anodal tDCS, cathodal tDCS and sham tDCS stimulation conditions were compared. MMN was defined as the peak negativity to deviant stimuli occurring within the 150–250 ms latency range in both experiments.

Our statistical analyses proceeded in two steps while auditory mismatch negativity and somatosensory mismatch negativity were run separately. First, to identify differences in scalp distribution between each condition, multivariate repeated measures analyses of variance were performed for each MMN component on nine leads (F3, Fz, F4, C3, Cz, C4, P3, Pz and P4). Data

were normalized across the nine leads and 10 subjects separately for every condition for this first step in order to equate amplitude differences between factors which might distort distribution effects (McCarthy & Wood, 1985). This resulted in a four-way repeated measures general linear model (GLM) on normalized data for localization with the factors laterality (3 levels: left, middle, right), anterior–posterior (3 levels: frontal, central, parietal), stimulation conditions (3 levels: anodal, cathodal, sham) and MMN timing (2 levels: pre and post). Having identified the electrode with the maximal effect of the MMN we then assessed, in a second step, stimulation condition and MMN timing effects on un-normalized data in a two-way repeated measures GLM. In these analyses, we focused only on the maximal effect electrode from the localization analyses. Finally, follow-up pairwise comparisons were run to assess the effect within levels of the stimulation or MMN timing factor. Only effects with sizes >0.35 (based on the intraclass correlation coefficient: ρ_{I}) were considered for follow-up analyses to avoid reporting non-essential effects. Greenhouse–Geisser-corrected results are reported when assumptions of sphericity were not met and Bonferroni correction was used for pairwise comparisons. The peak latency of MMN was later tested using the electrode selected by the peak amplitude. With the method as used for amplitude analysis, a two-way repeated measures GLM on un-normalized data for stimulation condition effects, MMN timing effects and interaction effect was run. In order to examine the possibility that differences in the MMN could be due to differences caused by a general alteration of standard ERPs and not by deviant detection (Umbricht *et al.* 2000, 2002; Korostenskaja *et al.* 2007), we also analysed the N60, P150 (Akatsuka *et al.* 2005; Spackman *et al.* 2010) components of the ERP to the standard sensory stimulus and N1, P2 components of the ERP to the standard auditory stimulus. The N1 component was defined as the most negative peak occurring in the 50–150 ms after stimulus onset and P2 as the most positive peak in the 150–250 ms after stimulus onset (Umbricht *et al.* 2002) while the N60 component was defined as the most negative peak in the 0–100 ms window and P150 as the most positive peak in the 100–200 ms window. The statistical analysis was the same as for MMN analysis.

To test if tDCS had differential effects on the amplitude of somatosensory MMN (sMMN) compared with auditory MMN (aMMN), an independent-samples *t* test was conducted to compare the ratio of amplitude change in MMN before and after anodal or cathodal simulation for the group where we recorded sMMN and the group where we recorded aMMN. The value of the ratio was derived from the peak amplitude of the post-stimulation recording divided by the peak amplitude of the pre-stimulation recording in each tDCS condition.

Results

Experiment 1

Spatial discrimination somatosensory MMN. We tried to replicate the spatial discrimination MMN, derived from subtraction of deviant from standard, published by Restuccia *et al.*, but there was no consistent MMN recordable across 10 subjects (Fig. 1*A*) in our laboratory setting. The averaged ERP component did not show conventional MMN morphology (Fig. 1*C*), although there was still a component of N60 visible predominantly in fronto-central leads.

Vibratory somatosensory MMN. A clear left fronto-central negative shift in the ERP responses to the deviant stimuli was observed between 150 and 250 ms following vibrotactile stimulus onset (sMMN) (Fig. 1), similar to that reported by others (Spackman *et al.* 2007, 2010; Butler *et al.* 2011, 2012). There was a good inter- and intra-subject reliability for this technique in producing MMN (Fig. 1*C*). We therefore used this technique to acquire sensory MMN for all subjects.

Of the 10 subjects tested, none was aware of the difference in stimulation type or sham stimulation nor did they report any side-effects except an itching sensation during the start of tDCS. The number of accepted trials was comparable between stimulation condition and between the MMN timing.

Figure 2*A* shows the grand average of MMN in each condition at the C3 electrode.

In a first step, a four-way repeated measures GLM for localization with normalization data (stimulation condition × MMN timing × anterior–posterior × laterality) was conducted to look for the electrodes with the largest MMN effects across conditions for later tests of the condition effects. We observed the largest MMN effect at the C3 electrode (anterior–posterior × laterality interaction; $F_{(4,36)} = 24.90$, $P < 0.00$, $\rho_{I} = 0.83$). As can be seen in Fig. 2, the distribution of the MMN did not differ across stimulation conditions (stimulation condition × anterior–posterior × laterality interaction; $F_{(8,72)} = 1.12$, $P = 0.36$) or MMN timing (pre–post × anterior–posterior × laterality interaction; $F_{(4,36)} = 0.46$, $P = 0.77$). Accordingly, we focused in a second step on the C3 electrode with non-normalized data for further two-way repeated measures GLM to assess the stimulation and timing effects. No reliable main effect of stimulation or MMN timing was observed ($F_{(1.29,11.58)} = 0.97$, $P = 0.37$; $F_{(1,9)} = 1.43$, $P = 0.26$). However, a significant stimulation condition × MMN timing interaction effect was observed ($F_{(2,18)} = 5.21$, $P < 0.02$, $\rho_{I} = 0.58$). As can be seen in Fig. 2*C*, pairwise comparison for stimulus conditions showed no MMN timing effect in the sham condition
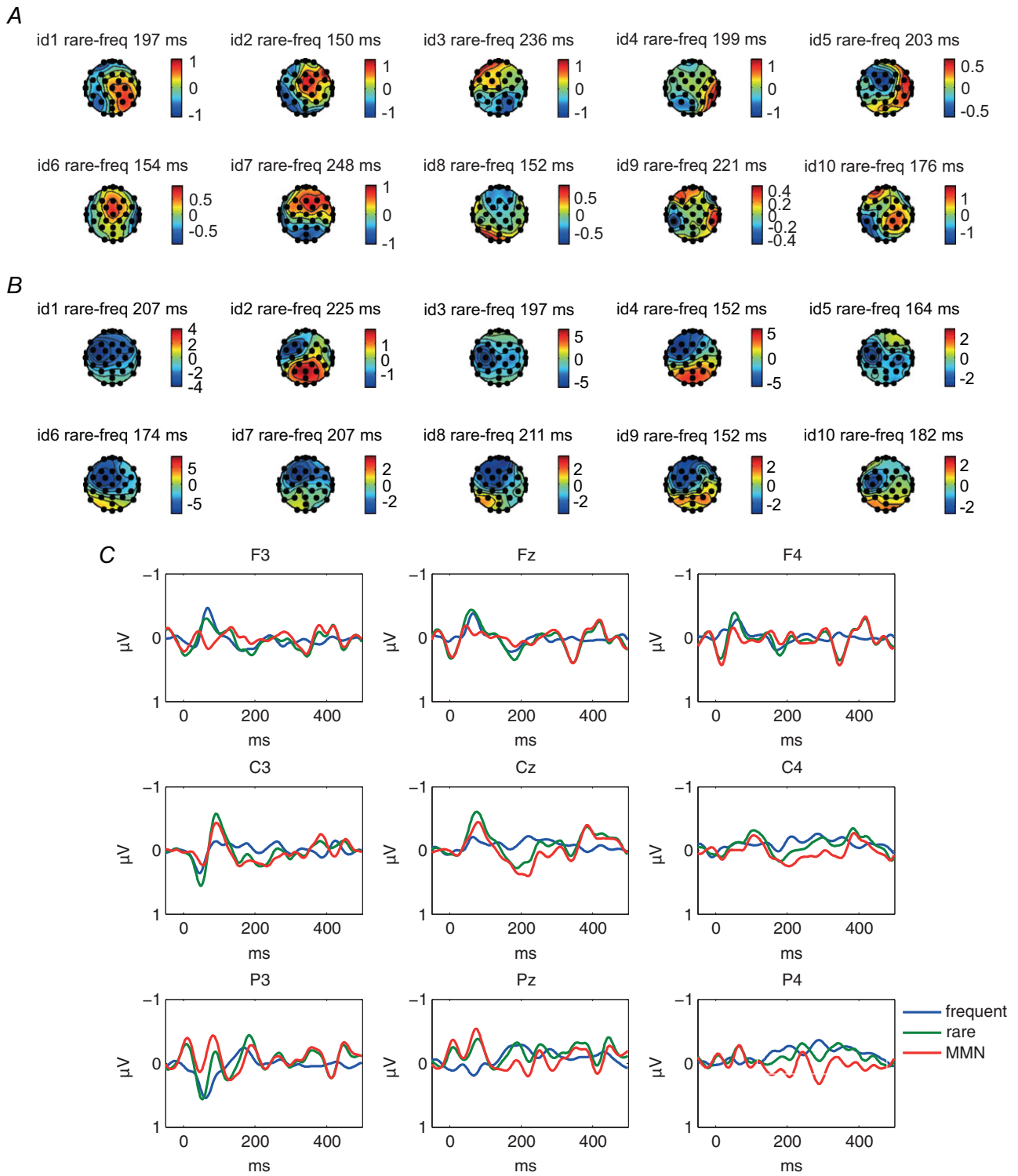
Figure 1.
Scalp topographies of 10 individual subjects of MMN ERPs in spatial discrimination condition (*A*) and vibratory condition (*B*). Maps are based on mean amplitudes of a 50 ms interval around individually defined MMN peaks in a time window of 150–250 ms after stimulus onset. Consistent central–frontal maxima of the MMN were noted only in vibratory sMMN. Grand average of standard, deviant and MMN ERPs at Fz, Cz and Pz in the spatial discrimination (*C*) and vibratory condition (*D*) across 10 subjects. A clear left fronto-central negative shift in the ERP responses to the deviant stimuli was observed between 150 and 250 ms following vibrotactile stimulus onset, but no reliable MMN was noted in spatial discrimination condition.

($F_{(1,9)} = 0.29$, $P = 0.61$), but a significant timing in the anodal condition ($F_{(1,9)} = 8.98$, $P < 0.02$, $\rho_I = 0.80$, mean difference anodal pre–post: -1.02 μV, SEM = 0.34) and cathodal condition ($F_{(1,9)} = 7.15$, $P < 0.03$, $\rho_I = 0.76$, mean difference cathodal pre–post: 0.65 μV, SEM = 0.24; Fig. 2*C*). The latency of the MMN showed no significant stimulation type or stimulation condition main effect, or stimulation condition × timing effect, at C3 (two-way repeated measures ANOVA: $F_{(2,18)} = 0.57$, $P = 0.88$; $F_{(1,9)} = 0.01$, $P = 0.93$; $F_{(2,18)} = 0.60$, $P = 0.58$; Fig. 2*D*).

Table 1 shows the peak amplitudes and latencies of N60 and P150 to standard stimuli before and after sham, anodal and cathodal conditions for the maximal effect electrode. With the method as used for MMN analysis, we first conducted a four-way repeated measures GLM for localization (stimulation condition × stimulus type × anterior–posterior × laterality) on normalized data to examine the electrodes with the largest N60 and P150 effects separately across conditions for later tests of the condition effects. We observed the largest N60 effect at the F3 electrode (anterior–posterior × laterality interaction; $F_{(4,36)} = 31.03$, $P < 0.00$, $\rho_I = 0.86$) and largest P150 at C3 electrode ($F_{(4,36)} = 14.52$, $P < 0.00$, $\rho_I = 0.73$). We focused on two-way repeated measures GLM on the maximal effect electrode to assess the stimulation condition and timing effects. There were no significant stimulation condition

or timing main effect or stimulation condition × timing interaction in N60 latencies, N60 amplitudes, P150 latencies or P150 amplitudes (Table 1).

Experiment 2

Auditory MMN. A MMN was observed after duration deviants. Figure 3*A* shows the grand average of MMN in each condition at the Fz electrodes. In a first step, a four-way repeated measures analysis of variance on normalized data was conducted to test for stimulation and condition differences in the scalp distribution of the MMN. In line with previous studies (Garrido *et al.* 2008), we observed the largest MMN effect at the Fz electrode (anterior–posterior × laterality interaction; $F_{(4,36)} = 10.01$, $P < 0.00$, $\rho_I = 0.64$). As can be seen in Fig. 3*B*, the distribution of the MMN did not differ across stimulation conditions (stimulation condition × anterior–posterior × laterality interaction; $F_{(8,72)} = 0.73$, $P = 0.67$) or MMN timing (pre–post × anterior–posterior × laterality interaction; $F_{(4,36)} = 0.62$, $P = 0.65$). Accordingly, we focused in a second step on the Fz electrode for further two-way repeated measures ANOVAs to assess the MMN timing and stimulation condition effects. No main effect of stimulation condition ($F_{(2,18)} = 0.33$, $P = 0.73$)
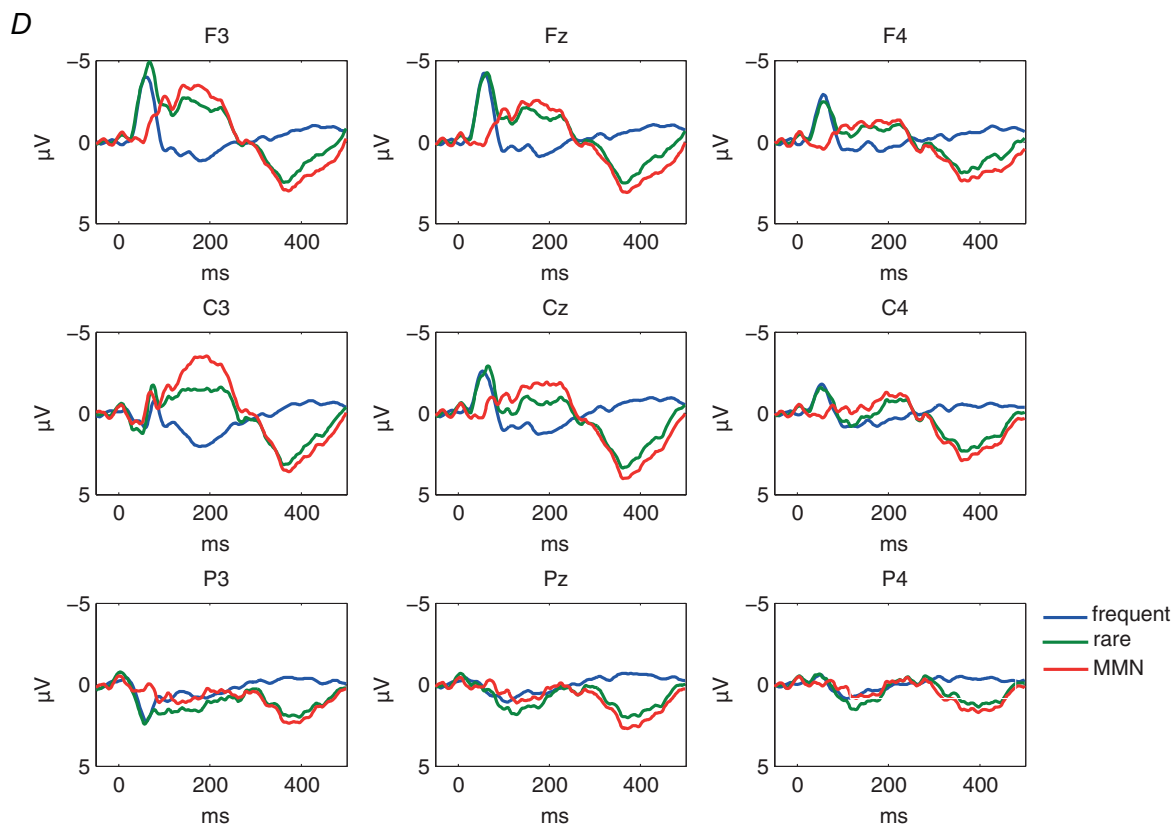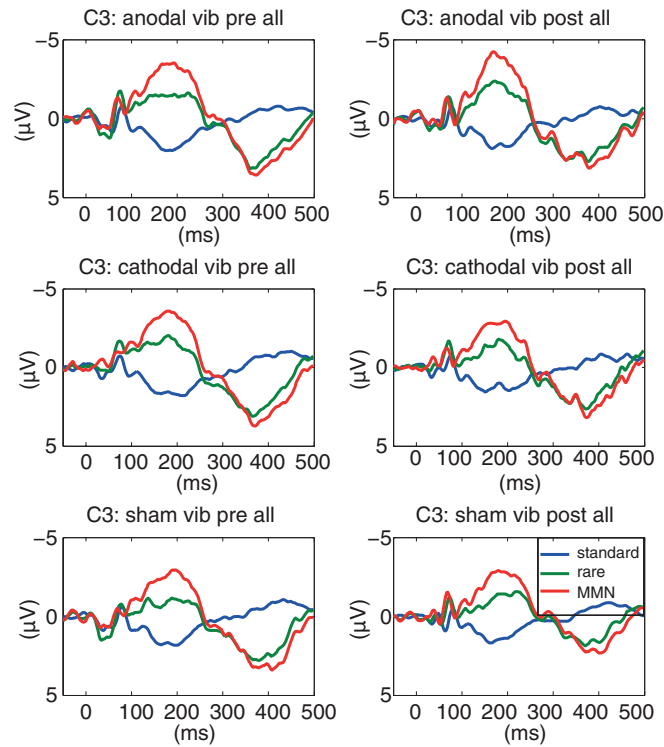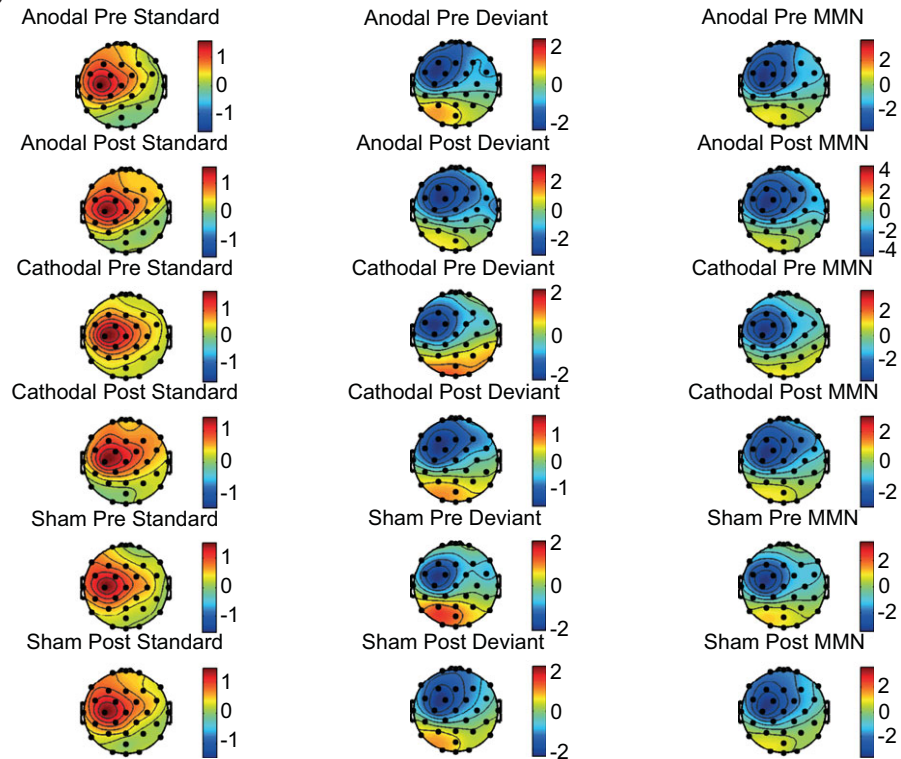

Figure 1. Continued

Figure 2.
A, grand average of standard, deviant and MMN ERPs at C3 in the vibratory testing across 10 subjects before and after sham, anodal and cathodal stimulation condition. *B*, scalp topographies of standard, deviant and MMN ERPs. Maps are based on mean amplitudes of a 50 ms interval around individually defined MMN peaks in a time window of 150–250 ms after stimulus onset. Consistent left central–frontal maximal effects of the MMNs were noted in each condition. *C*, MMN peak amplitudes before and after sham, anodal and cathodal tDCS

Table 1. Mean, standard deviation and repeated measures GLM of N1, P2 and N60, P150 peak latencies and amplitudes of standard ERP from aMMN and sMMN

	Anodal pre	Anodal post	Cathodal pre	Cathodal post	Sham pre	Sham post	Stimulation	Timing	Interaction
N60 amplitude	−4.1 ± 1.4	−4.2 ± 1.2	−4.4 ± 1.3	−4.5 ± 1.2	−4.2 ± 1.0	−3.7 ± 1.4	$F_{(2,18)} = 0.90\ P = 0.42$	$F_{(1,9)} = 0.15\ P = 0.71$	$F_{(2,18)} = 0.83,\ P = 0.45$
P150 amplitude	2.5 ± 0.9	2.6 ± 1.4	2.5 ± 0.9	2.5 ± 0.8	2.6 ± 1.2	2.7 ± 1.7	$F_{(2,18)} = 0.15\ P = 0.87$	$F_{(1,9)} = 0.19\ P = 0.67$	$F_{(2,18)} = 0.10,\ P = 0.90$
N60 latency	63 ± 11	58 ± 8	60 ± 7	60 ± 9	59 ± 6	57 ± 5	$F_{(2,18)} = 0.43\ P = 0.66$	$F_{(1,9)} = 2.53\ P = 0.15$	$F_{(2,18)} = 1.01,\ P = 0.38$
P150 latency	152.2 ± 45.7	145.2 ± 51.5	156.7 ± 58.9	150.5 ± 65.2	149.6 ± 47.0	146.2 ± 36.0	$F_{(2,18)} = 0.09\ P = 0.91$	$F_{(1,9)} = 0.39\ P = 0.55$	$F_{(2,18)} = 0.02,\ P = 0.98$
N1 amplitude	−0.7 ± 0.4	−0.7 ± 0.5	−0.6 ± 0.4	−0.7 ± 0.6	−0.8 ± 0.5	−0.8 ± 0.5	$F_{(2,18)} = 0.56\ P = 0.58$	$F_{(1,9)} = 0.00\ P = 0.96$	$F_{(2,18)} = 0.03,\ P = 0.97$
P2 amplitude	0.7 ± 0.2	0.7 ± 0.2	0.9 ± 0.4	0.8 ± 0.6	0.7 ± 0.3	0.8 ± 0.6	$F_{(2,18)} = 0.58\ P = 0.57$	$F_{(1,9)} = 0.25\ P = 0.63$	$F_{(2,18)} = 0.21,\ P = 0.82$
N1 latency	107.5 ± 14.1	106.1 ± 12.9	110.9 ± 22.8	107.3 ± 20.7	105.5 ± 13.7	106.6 ± 13.8	$F_{(2,18)} = 0.16\ P = 0.85$	$F_{(1,9)} = 0.14\ P = 0.71$	$F_{(2,18)} = 0.12,\ P = 0.89$
P2 latency	165 ± 20	165 ± 14	173 ± 19	160 ± 18	168 ± 13	169 ± 19	$F_{(2,18)} = 0.33\ P = 0.73$	$F_{(1,9)} = 1.36\ P = 0.27$	$F_{(2,18)} = 2.26,\ P = 0.13$

Before and after sham, anodal and cathodal stimulation were acquired at C3 in sMMN and Fz in aMMN. No significant differences between stimulation condition and timing were observed (cf. Results).

or MMN timing ($F_{(1,9)} = 0.01$, $P = 0.93$) was observed, nor a significant simulation condition × MMN timing interaction effect ($F_{(1.25,11.26)} = 0.25$, $P = 0.68$). The latency of auditory MMN also showed no main effect of

C

D
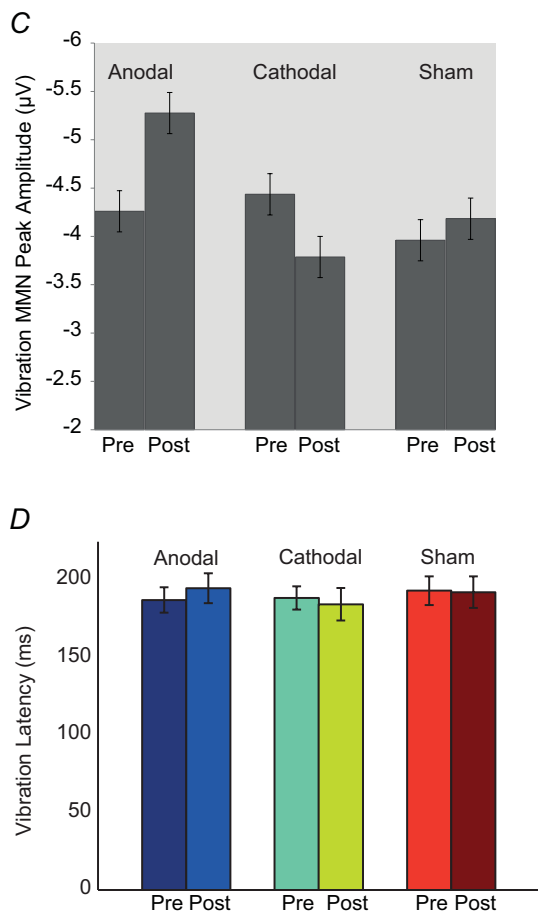
Figure 2. stimulation conditions for the vibratory stimulus condition at C3 electrode. *D*, MMN peak latencies before and after sham, anodal and cathodal tDCS stimulation conditions for the duration deviant condition at C3 electrode. Error bars indicate 1 SEM. MMN peak amplitudes after the anodal stimulation were significant larger whereas in the cathodal stimulation condition they were significantly smaller as compared to pre-stimulation conditions.

stimulation condition ($F_{(2,18)} = 0.45$, $P = 0.64$) or MMN timing ($F_{(1,9)} = 0.28$, $P = 0.61$), nor a significant MMN timing × stimulation condition effect at Fz (two-way repeated measures ANOVA, $F_{(2,18)} = 0.14$, $P = 0.87$; Fig. 3*D*). Table 1 shows the peak amplitudes and latencies of N1 and P2 to standard stimuli before and after sham, anodal and cathodal conditions for the maximal effect electrode. With the same method as in MMN analysis, we first conducted a four-way repeated measures GLM for localization (stimulation condition × stimulus type × anterior–posterior × laterality) on normalized data to examine the electrodes with the largest N1 and P2 effects separately across conditions for later tests of the condition effects. We observed the largest N1 effect at the Fz electrode (anterior–posterior × laterality interaction; $F_{(4,36)} = 10.00$, $P < 0.001$, $\rho_I = 0.64$) and largest P2 at Cz electrode ($F_{(4,36)} = 15.04$, $P < 0.001$, $\rho_I = 0.74$). We focused on two-way repeated measures GLM on the maximal effect electrode to assess the stimulation condition and timing effects. There was no significant stimulation condition or timing main effect, or stimulation condition × timing interaction in N1 latencies, N1 amplitudes, P2 latencies, or P2 amplitudes (Table 1).

To test whether tDCS had differential effects on the amplitude of somatosensory MMN but no effect on auditory MMN, a comparison between the two groups with the ratio of post/pre amplitude on sMMN and aMMN was conducted. There was a significant difference in the ratio for the anodal condition ($t_{(18)} = -2.30$, $P = 0.03$, mean ratio difference vibratory–auditory $= 0.35$, SEM $= 0.15$) and the cathodal condition ($t_{(18)} = -2.38$, $P = 0.04$, mean ratio difference vibratory–auditory $= -0.46$, SEM $= 0.19$). These results confirm that tDCS has an effect on sMMN but not on aMMN.

Discussion

Here we demonstrate that non-invasive brain stimulation with anodal and cathodal tDCS over the cerebellum is capable of increasing or reducing sMMN for duration

deviants. Anodal and cathodal tDCS, but not sham stimulation, had differential effects on the amplitude of sMMN but failed to have an effect on auditory MMN in the other group of subjects. This finding is consistent with previous reports of reduction in sMMN with cerebellar lesions, and the dissociation between effects on sMMN and aMMN is consistent with previous reports that there are different networks that generate these two phenomena (Molholm *et al.* 2005; Restuccia *et al.* 2007; Spackman *et al.* 2010; Butler *et al.* 2011). Our results extend these previous observations by demonstrating that the amplitude of sMMN can be enhanced as well as reduced, and that these effects can occur via the use of non-invasive brain stimulation in healthy subjects.

In contrast to aMMN, sMMN is much more rarely studied, and in keeping with this, models to explain its generation are less developed than for aMMN. It seems likely that a number of interconnected structures mediate sMMN as it appears they do for aMMN. The results of the current study and that of Restuccia *et al.* in patients with cerebellar lesions, clearly suggest that the cerebellum is an important node in this network. The fronto-central location of the sMMN potential would also be consistent with the suggestion that frontal regions, perhaps the same regions involved in aMMN such as the inferior frontal gyrus, form another important structure involved in generating sMMN.

Auditory MMN has been explained by both local plastic changes that reduce evoked responses to repeated stimuli (the adaptation hypothesis; Jaaskelainen *et al.* 2004) and a process involving message passing between interconnected structures whereby a memory trace for a repeated stimulus is compared with current sensory input (model adjustment hypothesis; Naatanen *et al.* 1992, 2005, 2007). If similar mechanisms underlie sMMN, then tDCS could exert its effect on both such mechanisms. tDCS is capable of producing an NMDA-dependent change in neuronal excitability that is thought to relate to long term potentiation (LTP) and long term depression (LTD) effects at synapses reported in direct electrical stimulation of animal brain slices (Purpura & McMurtry, 1965). tDCS has shown its efficacy in changing auditory MMN with cerebral stimulation (Chen *et al.* 2013) and cerebellar tDCS of the type we used in the current study is also capable of inducing behavioural effects in healthy human subjects in both motor adaptation (Galea *et al.* 2011) and in putative non-motor functions of the cerebellum (Ferrucci *et al.* 2008, 2012). In previous studies, anodal tDCS over the cerebellum increases the inhibition of cerebellum on motor cortex (as indexed by the transcranial magnetic stimulation measure 'cerebellar-brain inhibition'), and cathodal tDCS reduced this (Galea *et al.* 2009). From a behavioural standpoint, anodal tDCS over the cerebellum increased the speed of visuomotor adaptation (Galea *et al.* 2011). We speculate that anodal tDCS could enhance (via

an LTP-like effect) adaptive processes in the cerebellum related to repetitive presentation of standard stimuli, resulting in a larger amplitude MMN generated from connected frontal regions with presentation of an oddball stimulus. Cathodal tDCS, via an LTD-like effect, would tend to block this adaptive process to repeated standard stimuli, resulting in reduced MMN to oddball stimuli.

The role of the cerebellum in adaptation to error is most commonly considered behaviourally in the motor domain, for example adaptation of movement trajectories to visual or proprioceptive perturbations. The finding that cerebellar tDCS can produce changes in the processing of purely sensory information in a task without a motor component is therefore of interest. It is in keeping with a limited number of previous studies that have probed sensory function of the cerebellum, for example in signalling the absence of an expected sensory event (Tesche & Karhu, 2000) – something clearly linked to sMMN – and reduction in amplitude of frontal N24 and parietal P24 components of somatosensory evoked potentials in patients with unilateral hemispheric lesions (Restuccia *et al.* 2001). Thus, even though cerebellar lesions are not classically associated with sensory symptoms, they appear to be capable of causing deficits in sensory processing that can be detected using EEG and fMRI. This work has been complemented by a recent study demonstrating that patients with cerebellar degeneration were unable to recalibrate a spatiotemporal prediction related to a visual target, even though they performed similarly to controls on a baseline spatiotemporal prediction task (Roth *et al.* 2013). Cerebellar tDCS may be a method to experimentally manipulate cerebellar functional state in order to explore the behavioural correlates of sensory processing abnormalities such as those we have demonstrated here with regard to sMMN. It might in this way provide insights as to whether reduction in sMMN could explain any of the clinical deficits of patients with cerebellar lesions/degeneration.

We did not find spatially separated somatosensory stimuli to be a reliable method to produce sMMN. One possible explanation is that the stimulus intensity was too low. As described in the preliminary experiments in Restuccia *et al.* one of the most difficult technical issues in eliciting sMMN is the stimulus intensity where strong stimuli tend to catch the subject's attention while trivial stimuli are not able to elicit ERPs (Restuccia *et al.* 2009). In addition, the mean age of our sMMN group (57.5 years, range: 49–72 years) was older than in the Restuccia *et al.* study (43.6 years, range: 27–64 years). Although the age effect on MMN data is still ambiguous, this might be another issue of relevance to our results (Cheng *et al.* 2013). In contrast, vibrotactile stimulation, as reported by others (Kekoni *et al.* 1997; Shinozaki *et al.* 1998; Spackman *et al.* 2007, 2010; Butler *et al.* 2011, 2012), showed a clear fronto-central negative
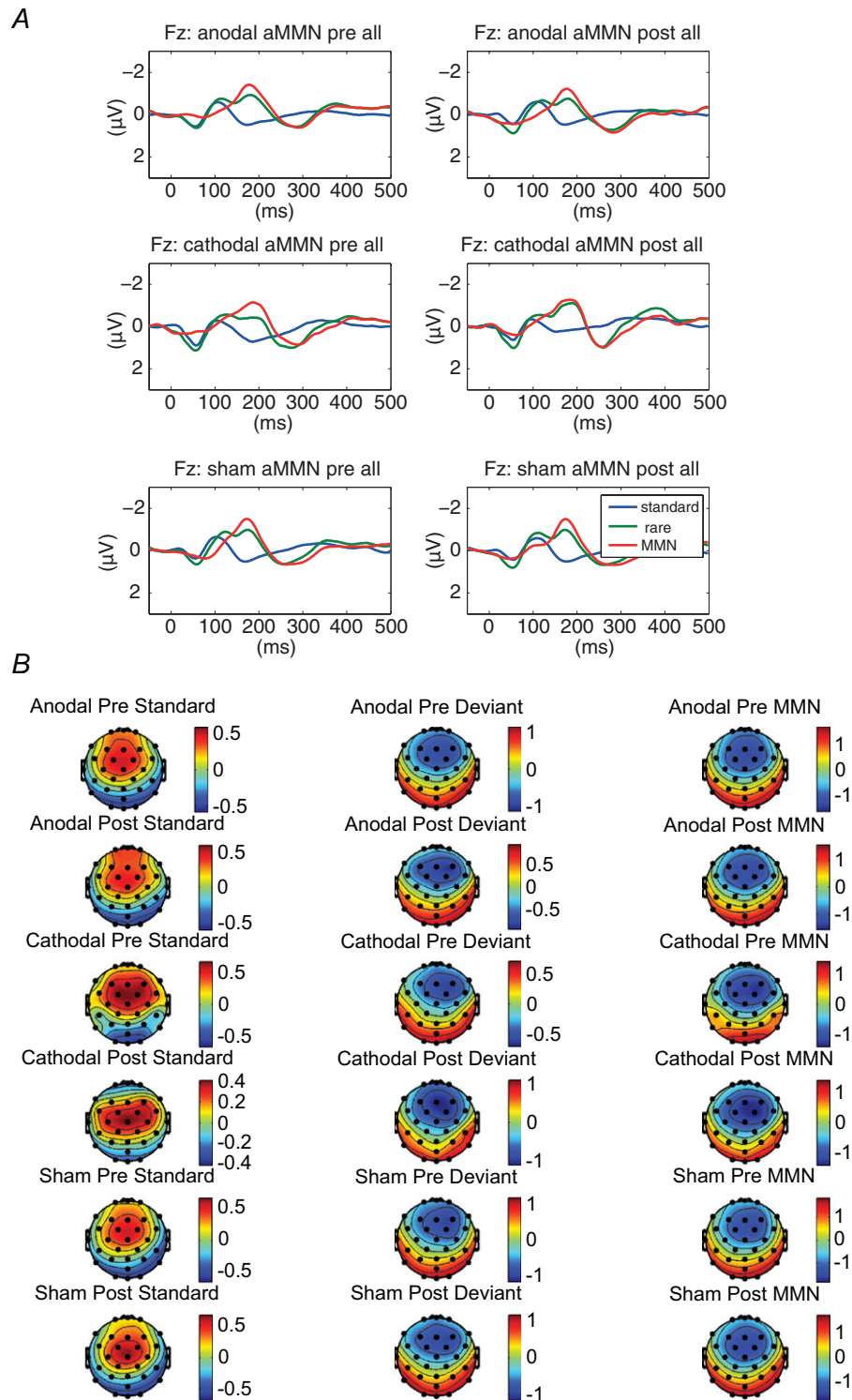
Figure 3.
A, grand average of standard, deviant and MMN ERP at Fz in auditory testing across 10 subjects before and after sham, anodal and cathodal stimulation conditions. *B*, scalp topographies of standard, deviant and MMN ERPs. Maps are based on mean amplitudes of a 50 ms interval around individually defined MMN peaks in a time window of 150–250 ms after stimulus onset. Consistent fronto-central maxima of the MMN were noted in each condition. *C*, MMN peak amplitudes before and after sham, anodal and cathodal tDCS stimulation conditions at Fz electrode. *D*, MMN peak latencies before and after sham, anodal and cathodal tDCS stimulation conditions for the duration deviant condition at Fz electrode. Error bars indicate 1 SEM. There are no differences in MMN peak amplitudes and latencies before and after sham, anodal or cathodal stimulation conditions.

shift in response to an infrequent change of vibration stimulus duration, which peaked around 150–250 ms, mimicking the MMN caused by auditory stimulation, and was predominant on the side contralateral to the stimulation side. The standard stimuli also showed a clear N60 component (Shinozaki *et al.* 1998).

Implications

There is clinical interest in the MMN given its absence in some neurological/neuropsychiatric disorders, most notably schizophrenia (Baldeweg *et al.* 2004), but also disorders of consciousness and amnesic syndromes. Though most studies in patient groups have assessed auditory MMN, it would be of interest to know if sMMN is also affected. At a more immediate level, tDCS offers a potentially valuable tool to manipulate sMMN in healthy people in order to assess mechanism and behavioural correlates with significant advantages over other methods that alter MMN experimentally, for example using the NMDA antagonist ketamine (Umbricht *et al.* 2000).
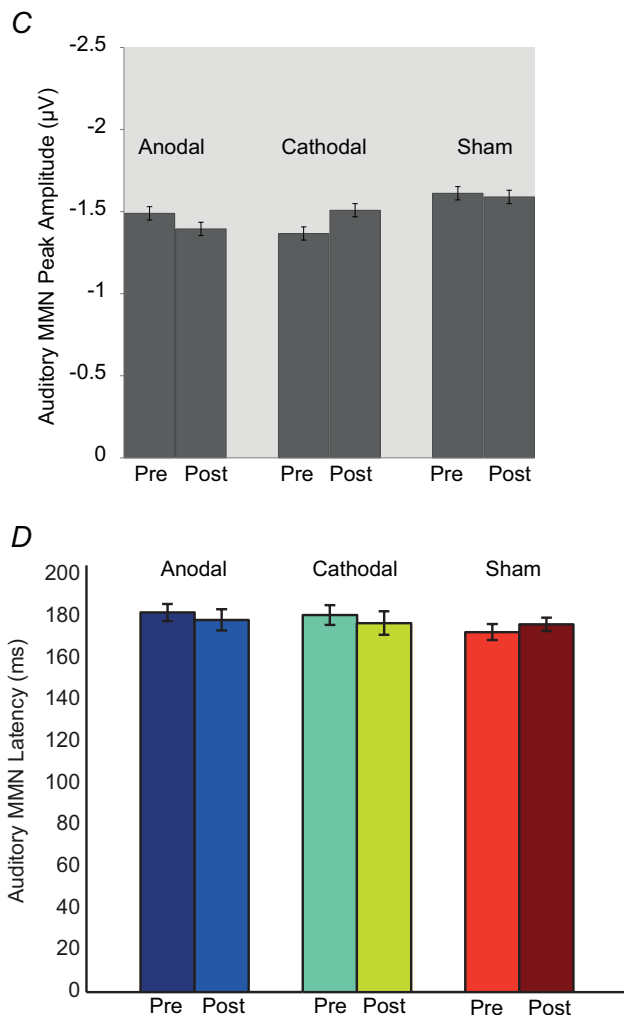

Conclusion

Modulation of cerebellar excitability by tDCS is capable of bidirectional modulation of somatosensory MMN, but has no effect on auditory MMN. This confirms the importance of the cerebellum in generating somatosensory MMN. In addition, we confirm that vibrotactile stimulation is a reliable way to evaluate sMMN in contrast to electrical stimulation.

References

Akatsuka K, Wasaka T, Nakata H, Inui K, Hoshiyama M & Kakigi R (2005). Mismatch responses related to temporal discrimination of somatosensory stimulation. *Clin Neurophysiol* **116**, 1930–1937.

Alho K, Woods DL, Algazi A & Naatanen R (1992). Intermodal selective attention. II. Effects of attentional load on processing of auditory and visual stimuli in central space. *Electroencephalogr Clin Neurophysiol* **82**, 356–368.

Baldeweg T, Klugman A, Gruzelier J & Hirsch SR (2004). Mismatch negativity potentials and cognitive impairment in schizophrenia. *Schizophr Res* **69**, 203–217.

Baldeweg T, Richardson A, Watkins S, Foale C & Gruzelier J (1999). Impaired auditory frequency discrimination in dyslexia detected with mismatch evoked potentials. *Ann Neurol* **45**, 495–503.

Butler JS, Foxe JJ, Fiebelkorn IC, Mercier MR & Molholm S (2012). Multisensory representation of frequency across audition and touch: high density electrical mapping reveals early sensory-perceptual coupling. *J Neurosci* **32**, 15338–15344.

Butler JS, Molholm S, Fiebelkorn IC, Mercier MR, Schwartz TH & Foxe JJ (2011). Common or redundant neural circuits for duration processing across audition and touch. *J Neurosci* **31**, 3400–3406.

Chen JC, Hämmerer D, Strigaro G, Liou LM, Tsai CH, Rothwell JC & Edwards MJ (2013). Domain-specific suppression of auditory mismatch negativity with transcranial direct current stimulation. *Clin Neurophysiol* (in press; DOI: 10.1016/j.clinph.2013.08.007).

Cheng CH, Hsu WY & Lin YY (2013). Effects of physiological aging on mismatch negativity: A meta-analysis. *Int J Psychophysiol* **90**, 165–171.

Ferrucci R, Giannicola G, Rosa M, Fumagalli M, Boggio PS, Hallett M, Zago S & Priori A (2012). Cerebellum and processing of negative facial emotions: cerebellar transcranial DC stimulation specifically enhances the emotional recognition of facial anger and sadness. *Cogn Emot* **26**, 786–799.

Ferrucci R, Marceglia S, Vergari M, Cogiamanian F, Mrakic-Sposta S, Mameli F, Zago S, Barbieri S & Priori A (2008). Cerebellar transcranial direct current stimulation impairs the practice-dependent proficiency increase in working memory. *J Cogn Neurosci* **20**, 1687–1697.

Friston KJ, Harrison L & Penny W (2003). Dynamic causal modelling. *Neuroimage* **19**, 1273–1302.

Figure 3. Continued

Galea JM, Jayaram G, Ajagbe L & Celnik P (2009). Modulation of cerebellar excitability by polarity-specific noninvasive direct current stimulation. *J Neurosci* **29**, 9115–9122.

Galea JM, Vazquez A, Pasricha N, de Xivry JJ & Celnik P (2011). Dissociating the roles of the cerebellum and motor cortex during adaptive learning: the motor cortex retains what the cerebellum learns. *Cereb Cortex* **21**, 1761–1770.

Garrido MI, Friston KJ, Kiebel SJ, Stephan KE, Baldeweg T & Kilner JM (2008). The functional anatomy of the MMN: a DCM study of the roving paradigm. *Neuroimage* **42**, 936–944.

Garrido MI, Kilner JM, Kiebel SJ, Stephan KE & Friston KJ (2007). Dynamic causal modelling of evoked potentials: a reproducibility study. *Neuroimage* **36**, 571–580.

Garrido MI, Kilner JM, Stephan KE & Friston KJ (2009). The mismatch negativity: a review of underlying mechanisms. *Clin Neurophysiol* **120**, 453–463.

Hamada M, Strigaro G, Murase N, Sadnicka A, Galea JM, Edwards MJ & Rothwell JC (2012). Cerebellar modulation of human associative plasticity. *J Physiol* **590**, 2365–2374.

Jaaskelainen IP, Ahveninen J, Bonmassar G, Dale AM, Ilmoniemi RJ, Levanen S, Lin FH, May P, Melcher J, Stufflebeam S, Tiitinen H & Belliveau JW (2004). Human posterior auditory cortex gates novel sounds to consciousness. *Proc Natl Acad Sci U S A* **101**, 6809–6814.

Kassavetis P, Saifee TA, Sadnicka A, Parees I, Kojovic M, Rothwell JC & Edwards MJ (2012). Adaptation of surround inhibition in the human motor system. *Exp Brain Res* **222**, 211–217.

Kekoni J, Hamalainen H, Saarinen M, Grohn J, Reinikainen K, Lehtokoski A & Naatanen R (1997). Rate effect and mismatch responses in the somatosensory system: ERP-recordings in humans. *Biol Psychol* **46**, 125–142.

Korostenskaja M, Nikulin VV, Kicic D, Nikulina AV & Kahkonen S (2007). Effects of NMDA receptor antagonist memantine on mismatch negativity. *Brain Res Bull* **72**, 275–283.

McCarthy G & Wood CC (1985). Scalp distributions of event-related potentials: an ambiguity associated with analysis of variance models. *Electroencephalogr Clin Neurophysiol* **62**, 203–208.

Molholm S, Martinez A, Ritter W, Javitt DC & Foxe JJ (2005). The neural circuitry of pre-attentive auditory change-detection: an fMRI study of pitch and duration mismatch negativity generators. *Cereb Cortex* **15**, 545–551.

Mowszowski L, Hermens DF, Diamond K, Norrie L, Hickie IB, Lewis SJ & Naismith SL (2012). Reduced mismatch negativity in mild cognitive impairment: associations with neuropsychological performance. *J Alzheimers Dis* **30**, 209–219.

Naatanen R, Jacobsen T & Winkler I (2005). Memory-based or afferent processes in mismatch negativity (MMN): a review of the evidence. *Psychophysiology* **42**, 25–32.

Naatanen R, Paavilainen P, Rinne T & Alho K (2007). The mismatch negativity (MMN) in basic research of central auditory processing: a review. *Clin Neurophysiol* **118**, 2544–2590.

Naatanen R, Teder W, Alho K & Lavikainen J (1992). Auditory attention and selective input modulation: a topographical ERP study. *Neuroreport* **3**, 493–496.

Paavilainen P, Karlsson ML, Reinikainen K & Naatanen R (1989). Mismatch negativity to change in spatial location of an auditory stimulus. *Electroencephalogr Clin Neurophysiol* **73**, 129–141.

Purpura DP & McMurtry JG (1965). Intracellular activities and evoked potential changes during polarization of motor cortex. *J Neurophysiol* **28**, 166–185.

Restuccia D, Della Marca G, Valeriani M, Leggio MG & Molinari M (2007). Cerebellar damage impairs detection of somatosensory input changes. A somatosensory mismatch-negativity study. *Brain* **130**, 276–287.

Restuccia D, Valeriani M, Barba C, Le Pera D, Capecci M, Filippini V & Molinari M (2001). Functional changes of the primary somatosensory cortex in patients with unilateral cerebellar lesions. *Brain* **124**, 757–768.

Restuccia D, Zanini S, Cazzagon M, Del Piero I, Martucci L & Della Marca G (2009). Somatosensory mismatch negativity in healthy children. *Dev Med Child Neurol* **51**, 991–998.

Roth MJ, Synofzik M & Lindner A (2013). The cerebellum optimizes perceptual predictions about external sensory events. *Curr Biol* **23**, 930–935.

Sams M, Paavilainen P, Alho K & Naatanen R (1985). Auditory frequency discrimination and event-related potentials. *Electroencephalogr Clin Neurophysiol* **62**, 437–448.

Shinozaki N, Yabe H, Sutoh T, Hiruma T & Kaneko S (1998). Somatosensory automatic responses to deviant stimuli. *Brain Res Cogn Brain Res* **7**, 165–171.

Spackman LA, Boyd SG & Towell A (2007). Effects of stimulus frequency and duration on somatosensory discrimination responses. *Exp Brain Res* **177**, 21–30.

Spackman LA, Towell A & Boyd SG (2010). Somatosensory discrimination: an intracranial event-related potential study of children with refractory epilepsy. *Brain Res* **1310**, 68–76.

Tervaniemi M, Maury S & Naatanen R (1994). Neural representations of abstract stimulus features in the human brain as reflected by the mismatch negativity. *Neuroreport* **5**, 844–846.

Tesche CD & Karhu JJ (2000). Anticipatory cerebellar responses during somatosensory omission in man. *Hum Brain Mapp* **9**, 119–142.

Umbricht D, Koller R, Schmid L, Skrabo A, Grubel C, Huber T & Stassen H (2003). How specific are deficits in mismatch negativity generation to schizophrenia? *Biol Psychiatry* **53**, 1120–1131.

Umbricht D, Koller R, Vollenweider FX & Schmid L (2002). Mismatch negativity predicts psychotic experiences induced by NMDA receptor antagonist in healthy volunteers. *Biol Psychiatry* **51**, 400–406.

Umbricht D, Schmid L, Koller R, Vollenweider FX, Hell D & Javitt DC (2000). Ketamine-induced deficits in auditory and visual context-dependent processing in healthy volunteers: implications for models of cognitive deficits in schizophrenia. *Arch Gen Psychiatry* **57**, 1139–1147.

Wijnen VJ, van Boxtel GJ, Eilander HJ & de Gelder B (2007). Mismatch negativity predicts recovery from the vegetative state. *Clin Neurophysiol* **118**, 597–605.

Yabe H, Tervaniemi M, Reinikainen K & Naatanen R (1997). Temporal window of integration revealed by MMN to sound omission. *Neuroreport* **8**, 1971–1974.

Additional information

Competing interests

None declared.

Author contributions

J.-C.C. and M.J.E. conceived and designed the experiments. J.-C.C. collected the data. All authors participated in the analysis and interpretation of the data and in the drafting of the manuscript. All authors approved the final version of the manuscript. Experiments were carried out at the Sobell Department of Motor Neuroscience and Movement Disorders, UCL Institute of Neurology.